

Product Control in Conversion of Ethanol on MIL-101(Cr) with Adjustable Brønsted Acid Density

Zheng Ming,^[a, b, c] Yingli Wang,^[b] Tiexin Zhang,^[c] Lingyun Li,^[b] Chunying Duan,^{*,[a, c]} and Zhongmin Liu^{*,[a, b]}

MIL-101(Cr) with adjustable Brønsted acid density was prepared via post-synthetic sulfation strategy, which was carried out with sulfuric acid in the presence of trifluoromethanesulfonic anhydride, using nitromethane as solvent. XRD, TG, EDS, XPS, IR, NH₃-TPD and acid-base titration were used to characterize structure and acidity. Adopting conversion of ethanol as a

probe reaction, gas-solid catalytic characteristics on MIL-101(Cr) and post-synthetic sulfated MIL-101(Cr) in a micro fixed-bed reactor were studied by continuous feeding. Combined with the regulation of reaction parameters, selective production of ethylene (100%) or diethyl ether (99%) could be achieved.

Introduction

Metal-organic framework (MOF)^[1] was a newly developed series of crystalline porous material self-assembled by metal ions and organic ligands. They had aroused keen interest of academia and industry due to their multiple potential adhibition on gas storage,^[2] separation,^[3] sensing^[4] and catalysis.^[5] Comparison with conventional porous material such as zeolite and mesoporous silicamaterial,^[6] MOF possessed the advantageous characteristics of more variable structures,^[7] much stronger designability^[8] and porosity adjustability,^[8d,9] larger surface areas,^[10] artful immobilization of guest species,^[11] precisely and orderly located atoms.^[12] Such characteristics made it possible to serve MOF as a new type of highly selective catalyst where functional sites could be designed precisely^[13] at the molecular level.

Over the past decades, unsaturated coordination metal sites or open metal sites on secondary building units (SBUs) of MOF were made and applied in catalysis,^[14] which served not only as structural building units, but also Lewis acid used as catalytic sites. For example, MIL-101(M) [M₃X(H₂O)₂O(BDC)₃; M=Al, Cr, Fe; X=F, OH; BDC=benzene-1,4-dicarboxylate] were found to be catalytically active in citronellal cyclization,^[15] aldehyde cyanosilylation,^[16] and selective oxidation of organic

compounds.^[17] A large amount of works on the catalytic properties of Lewis acidic MOF had been done in recent years.

By contrast, study of Brønsted acidic MOF was just at its initial stage.^[18] So far, there were three main methods to prepare Brønsted acidic MOF. One way was to encapsulate protonic acid molecules (e.g. polyoxometalates,^[19] H₂SO₄ and H₃PO₄^[20]), which might cause channel blockage and the leaching of encapsulated molecules. Another method was to bound proton compounds such as H₂O, ROH, HOCCOOH and H₂SO₄^[21] directly to metal sites, which would consume Lewis acid and usually get unstable Brønsted acid. The most extensively studied approach was to covalently graft functional group containing active hydrogen such as –NH₃⁺,^[22] –SO₃H,^[23] –COOH^[24] on organic linking units, thereinto grafted –SO₃H group had aroused much interest and shown great catalytic potential of Brønsted acidic MOF due to its strong Brønsted acidity.^[18,25]


Brønsted acid catalysis was widely used in industrial catalytic process, such as methanol to hydrocarbons^[26] and C₂H₅OH dehydration.^[27] Within the precisely located active sites, Brønsted acidic MOF had the potential application in such industrial catalytic process. But so far, the published works in this field mainly focused on fundamental research under mild reaction conditions^[28] in liquid-phase batch reactor. Researchers paid more attention to active phase attribution and mechanism deduction. Few studies were concerned with gas-solid catalytic characteristics, which was close to the actual industrial production process.^[18]

In this work, MIL-101(Cr), a kind of MOF with relatively good thermal stability, was used as the starting material. After post-synthetic sulfation, MIL-101(Cr) with adjustable Brønsted acid density was prepared. Adopted conversion of C₂H₅OH as a probe reaction, gas-solid catalytic characteristics on MIL-101(Cr) and post-synthetic sulfated MIL-101(Cr) were studied in a micro fixed-bed reactor by continuous feeding. Effect of adjustable acidity on product distribution were investigated. C₂H₅OH was an important industrial raw material, mainly produced from biomass and coal,^[29] which was used for production of C₂H₄^[27] as a building block of polyolefins,^[30] C₂H₅OC₂H₅ and

[a] Z. Ming, Prof. C. Duan, Prof. Z. Liu
Zhang Dayu College of Chemistry
Dalian University of Technology
Dalian 116024 (P. R. China)
E-mail: cyduan@dlut.edu.cn
liuzm@dicp.ac.cn

[b] Z. Ming, Prof. Y. Wang, L. Li, Prof. Z. Liu
National Engineering Laboratory for Methanol to Olefins
Dalian National Laboratory for Clean Energy
Dalian Institute of Chemical Physics
Chinese Academy of Sciences
Dalian 116023 (P. R. China)

[c] Z. Ming, Prof. T. Zhang, Prof. C. Duan
State Key Laboratory of Fine Chemicals
Dalian University of Technology
Dalian 116024 (P. R. China)

 Supporting information for this article is available on the WWW under <https://doi.org/10.1002/cctc.202001346>

CH₃COOC₂H₅ as common solvents,^[31] and CH₃CHO as feedstock for spices, medicines and agricultural chemicals.^[32]

Results and Discussion

The as-synthesized samples exhibited characteristic diffraction peaks conformed to the data for MIL-101 in published works,^[10a,25a] as shown in Figure 1a (Small-angle XRD patterns) and Figure 1b (XRD patterns). After post-synthetic sulfation, diffraction peaks intensity at $2\theta = 3^\circ$ and 8° increased obviously, demonstrating that long-term order of large interfacial spacing structure was improved, which might be ascribed to the elution of free organic ligands and Cr salt in MIL-101(Cr) after post-synthetic sulfation. The as-synthesized MIL-101(Cr) exhibited a typical octahedral crystal with a uniform crystallite size of 500 nm (Figure 1c). No change in the morphology was observed after post-synthetic sulfation (Figure 1d~1f). Figure 1g showed IR spectra of MIL-101(Cr) and post-synthetic sulfated MIL-101(Cr). New bands appeared at 1170 cm^{-1} and 1260 cm^{-1} on post-synthetic sulfated MIL-101(Cr), which could be ascribed to O=S=O symmetric and asymmetric stretching modes.^[33] The bands at 1030 cm^{-1} and 1230 cm^{-1} could be assigned to the S–O stretching vibration and C–O stretching vibration of phenol derivatives respectively. And the band at 1110 cm^{-1} belonged to the in-plane skeletal vibration of substituted benzene.^[25a,33b,34] Results testified –OSO₃H group was grafted on BDC after post-synthetic sulfation.

Figure 1h showed XPS spectra of MIL-101(Cr) and post-synthetic sulfated MIL-101(Cr). As Cr2p narrow-scan spectra shown in the upper part, valence state of Cr had not changed after post-synthetic sulfation, which indicated that there might be no coordination between Cr and –OSO₃H group. As survey-scan spectra shown, Sulfur element was observed on the post-synthetic sulfated MIL-101(Cr). And S2p peak intensity of LS-MIL-101(Cr), S-MIL-101(Cr) and HS-MIL-101(Cr) increased successively. In order to represent the composition of grafted –OSO₃H group on BDC quantitatively, a new parameter S/Cr ratio was proposed due to a certain coordination number of Cr with BDC in MIL-101(Cr). As shown in Table 1, bulk S/Cr ratio from EDS was 0.28, 0.30 and 0.44, and surface S/Cr ratio from XPS was 0.52, 0.82 and 0.87 on LS-MIL-101(Cr), S-MIL-101(Cr) and HS-MIL-101(Cr), respectively. Results indicated that the composition of grafted –OSO₃H group was increased gradually with the increasing of $n[\text{H}_2\text{SO}_4]:n[\text{BDC}]$, and the composition of grafted –OSO₃H group on the surface was significantly higher than that in bulk phase, which testified a sulfur-rich surface was formed after post-synthetic sulfation.

Figure 1i showed TGA results of MIL-101(Cr) and post-synthetic sulfated MIL-101(Cr). For all samples, a weight loss of 19% was shown in the initial stage, corresponding to physical

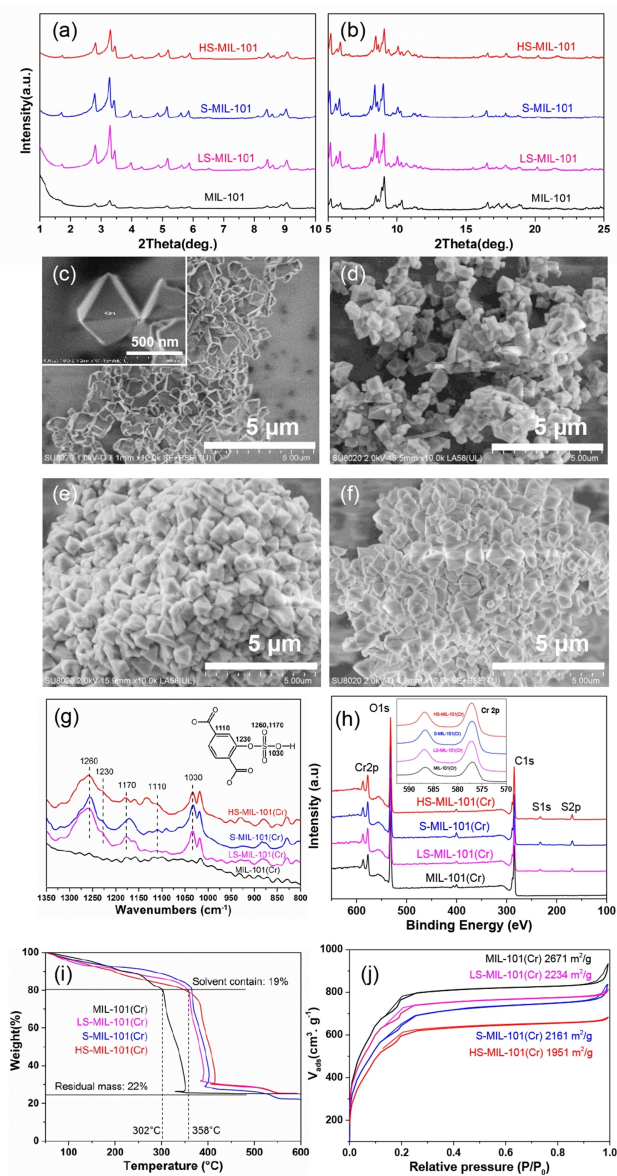


Figure 1. Small-angle XRD patterns(a) and XRD patterns (b) of MIL-101(Cr) and post-synthetic sulfated MIL-101(Cr); SEM photos of MIL-101(Cr) (c), LS-MIL-101(Cr) (d), S-MIL-101(Cr) (e) and HS-MIL-101(Cr) (f); IR spectra (g), XPS spectra (h), TGA analysis (i), and nitrogen sorption isotherms (j) of MIL-101(Cr) and post-synthetic sulfated MIL-101(Cr).

Table 1. Post-synthetic sulfated conditions and quantitative analysis results.

Sample	MIL-101(Cr)	LS-MIL-101(Cr)	S-MIL-101(Cr)	HS-MIL-101(Cr)
$n[\text{H}_2\text{SO}_4]:n[\text{BDC}]$	–	0.5:1	1.25:1	4:1
Agitating time [min]	–	60	100	100
Bulk S/Cr ratio from EDS	0	0.28	0.30	0.44
Surface S/Cr ratio from XPS	0	0.52	0.82	0.87
Total acid density from NH ₃ –TPD [mmol/g]	0.71	0.49	0.56	1.08
Brønsted acid density from titration [mmol/g]	0	0.22	0.27	0.42

adsorption of residual organic solvent and H₂O. Then, MIL-101 (Cr) exhibited a rapid weight loss at 300 °C, due to framework dissociation. After post-synthetic sulfation, the starting temperature of framework dissociation rose to 350 °C, which indicated that improvement of framework integrity might help to enhance thermal stability of MIL-101(Cr). Therefore, pretreatment temperature and reaction temperature in the subsequent reactions and characteristics was not allowed to exceed 250 °C. Nitrogen sorption isotherms of MIL-101(Cr) and post-synthetic sulfated MIL-101(Cr) were depicted in Figure 1j. The shape of the isotherms remained unchanged after post-synthetic sulfation, while specific surface area was decreased from 2671 m²/g for MIL-101(Cr) to 2234, 2161 and 1951 m²/g for LS-MIL-101(Cr), S-MIL-101(Cr) and HS-MIL-101(Cr), respectively, which was consistent with the gradually increasing composition of grafted –OSO₃H group in EDS and XPS results.

NH₃-TPD and NH₃-TPD-MS profiles of MIL-101(Cr) and post-synthetic sulfated MIL-101(Cr) were illustrated in Figure 2a and 2b. The experiment was conducted below 250 °C in order to avoid signal interference caused by thermal decomposition. Only one desorption peak at 130 °C was observed on MIL-101 (Cr), which was attributed to NH₃ desorption at open Cr site of Lewis acid. As shown in previous report,^[28] six-coordinated metal sites in MIL-101(Cr) were partially in coordination with other ligands such as organic solvents and H₂O, which could be removed in the pretreatment process to form open metal sites. A new desorption peak at 210 °C appeared on post-synthetic sulfated MIL-101(Cr), which might be ascribed to NH₃ desorption from grafted –OSO₃H group. As IR spectra of NH₃ adsorption shown in Figure S1, vibrations of NH₄⁺(δ_{asym}), the corresponding species formed by NH₃ adsorbed on Brønsted acid, was observed on post-synthetic sulfated MIL-101(Cr) at 1480 cm⁻¹, which testified grafted –OSO₃H group performed as Brønsted acid definitely. Brønsted acid density determined by Acid-Base titration and total acid density determined by NH₃-

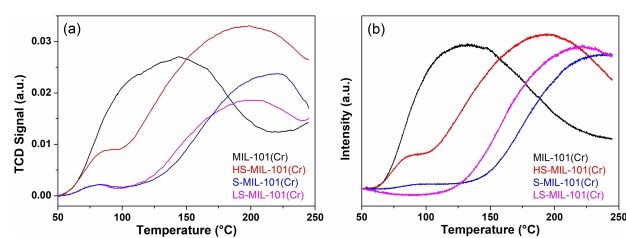


Figure 2. NH₃-TPD (a) and NH₃-TPD-MS (b) of MIL-101(Cr) and post-synthetic sulfated MIL-101(Cr).

TPD was listed in Table 1. Total acid density decreased first and then increased due to the elution of free Cr salt in MIL-101(Cr) after post-synthetic sulfation, while Brønsted acid density was 0.22, 0.27 and 0.42 on LS-MIL-101(Cr), S-MIL-101(Cr) and HS-MIL-101(Cr), respectively, which testified Brønsted acid density could be adjusted with the increasing of $n[\text{H}_2\text{SO}_4]:n[\text{BDC}]$ after post-synthetic sulfated. Considering the formation of sulfur-rich surface from EDS and XPS, more Brønsted acid located at the external surface on post-synthetic sulfated MIL-101(Cr).

Conversion of C₂H₅OH on MIL-101(Cr) and post-synthetic sulfated MIL-101(Cr). Table 2 showed catalytic performance in conversion of C₂H₅OH on MIL-101(Cr) and post-synthetic sulfated MIL-101(Cr). In terms of reaction pathways, two kinds of product were derived. One was dehydration products including C₂H₄ and C₂H₅OC₂H₅, another was dehydrogenation products including CH₃CHO and CH₃COOC₂H₅, thereinto, CH₃COOC₂H₅ was secondary product of dehydrogenated species CH₃COOH further reacted with C₂H₅OH, which was usually referred to as rapid esterification reaction. In this work, CH₃COOC₂H₅ instead of CH₃COOH was ascribed to dehydrogenated product. Results indicated that there might be five main reaction processes in conversion of C₂H₅OH on post-synthetic sulfated MIL-101(Cr): (1) Intramolecular Dehydration: C₂H₅OH=C₂H₄+H₂O; (2) Intermolecular Dehydration: 2 C₂H₅OH=C₂H₅OC₂H₅+H₂O (3) Dehydrogenation: C₂H₅OH=CH₃CHO+H₂; (4) Oxidative Dehydrogenation: C₂H₅OH+H₂O=CH₃COOH+2H₂; (5) Esterification: C₂H₅OH+CH₃COOH=CH₃COOC₂H₅+H₂O. By-products H₂O and H₂ were not included in the quantitative results in product distribution.

As shown in Table 2, MIL-101(Cr) and post-synthesized sulfated MIL-101(Cr) exhibited excellent performance in conversion of C₂H₅OH. Under the continuous feeding of C₂H₅OH, C₂H₅OH conversion of 43.4% was observed on MIL-101(Cr). After post-synthetic sulfation, C₂H₅OH conversion was 28.7%, 36.5% and 77.4% on LS-MIL-101(Cr), S-MIL-101(Cr) and HS-MIL-101(Cr), respectively. The trend of C₂H₅OH conversion was essentially in agreement with that of total acid density, as shown in Table 1, which indicated that both open Cr site of Lewis acid and grafted –OSO₃H group of Brønsted acid showed positive effect in conversion of C₂H₅OH.

In terms of product distribution, selectivity of dehydrogenation products (CH₃CHO and CH₃COOC₂H₅) on MIL-101(Cr) was 99.4%, and only trace amount of C₂H₅OC₂H₅ was obtained, which indicated that open Cr site of Lewis acid acted as dehydrogenation center. With the increasing composition of grafted –OSO₃H group, selectivity of dehydrated products (C₂H₄ and C₂H₅OC₂H₅) increased gradually, which was 9.8%, 69.9%

Table 2. Catalytic performance in conversion of C₂H₅OH on MIL-101(Cr) and post-synthetic sulfated MIL-101(Cr).^[a]

Catalysts	Conversion [%]	Selectivity[%]			
		C ₂ H ₄	CH ₃ CHO	C ₂ H ₅ OC ₂ H ₅	CH ₃ COOC ₂ H ₅
MIL-101(Cr)	43.4	0	95.3	0.6	4.1
LS-MIL-101(Cr)	28.7	4.3	86.4	5.5	3.8
S-MIL-101(Cr)	36.5	40.3	26.9	29.6	3.2
HS-MIL-101(Cr)	77.4	65.1	7.5	27.2	0.2

[a] Product distribution at TOS(time on stream) = 230 min, reaction temperature = 250 °C, WHSV = 0.02 h⁻¹.

and 92.3% on LS-MIL-101(Cr), S-MIL-101(Cr) and HS-MIL-101(Cr), respectively. Results indicated that grafted $-\text{OSO}_3\text{H}$ group of Brønsted acid might act as dehydration center. It was worth noting that selectivity of dehydrated products on S-MIL-101(Cr) was much higher than that on LS-MIL-101(Cr), both of which possessed similar Brønsted acid density. Possible reason was the formation of sulfur-rich surface on S-MIL-101(Cr), which enhanced the accessibility of Brønsted acid.

Effect of reaction temperature on product distribution. Figure 3 showed $\text{C}_2\text{H}_5\text{OH}$ conversion and product distribution as a function of reaction temperature on S-MIL-101(Cr). With the increasing of reaction temperature, $\text{C}_2\text{H}_5\text{OH}$ conversion on S-MIL-101(Cr) increased. In terms of product distribution, selectivity of CH_3CHO and selectivity of $\text{CH}_3\text{COOC}_2\text{H}_5$ increased, while selectivity of $\text{C}_2\text{H}_5\text{OC}_2\text{H}_5$ decreased continuously, and selectivity of C_2H_4 increased first and then decreased. Results showed that lower reaction temperature was beneficial to intermolecular dehydration reaction on grafted $-\text{OSO}_3\text{H}$ group

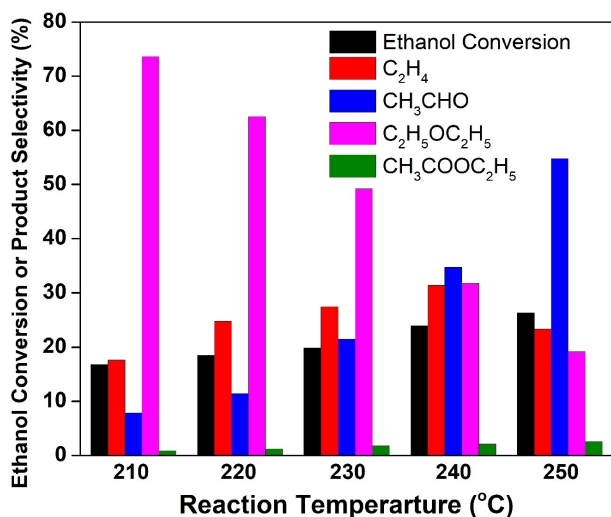


Figure 3. $\text{C}_2\text{H}_5\text{OH}$ Conversion and product distribution as a function of reaction temperature on S-MIL-101(Cr) (WHSV = 0.02 h^{-1} , TOS = 600 min).

of Brønsted acid, while higher reaction temperature was favorable for intramolecular dehydration reaction on grafted $-\text{OSO}_3\text{H}$ group of Brønsted acid and dehydrogenation reaction on open Cr site of Lewis acid.

Effect of $\text{C}_2\text{H}_5\text{OH}$ concentration on product distribution. In this work of Gas-solid reaction on MOF, zero point in conversion of $\text{C}_2\text{H}_5\text{OH}$ was designated as the moment when $\text{C}_2\text{H}_5\text{OH}$ was fed into the reactor carried with N_2 . As a large adsorption capacity material, surface $\text{C}_2\text{H}_5\text{OH}$ concentration on MOF would accumulate in the initial stage. After equilibrium adsorption capacity was reached, conversion of $\text{C}_2\text{H}_5\text{OH}$ proceeded to steady-state reaction stage. This was the main reason why TOS = 230 min was used to analyze catalytic performance in the above work.

Figure 4 showed $\text{C}_2\text{H}_5\text{OH}$ adsorbance (Figure 4a) and GC-FID chromatograms (Figure 4b) as a function of TOS in the initial stage. $\text{C}_2\text{H}_5\text{OH}$ adsorbance was used as a quantitative expression of surface $\text{C}_2\text{H}_5\text{OH}$ concentration, which was estimated using the feeding molar mass minus the converting and discharging molar mass. When TOS = 5 min, $\text{C}_2\text{H}_5\text{OH}$ adsorbance on HS-MIL-101(Cr) was 0.04 mmol/g, C_2H_4 was the only reaction product, which indicated that $\text{C}_2\text{H}_5\text{OH}$ adsorbed on grafted $-\text{OSO}_3\text{H}$ group of Brønsted acid preferentially, selectivity of C_2H_4 could be highly improved in a lower surface $\text{C}_2\text{H}_5\text{OH}$ concentration. A small amount of CH_3CHO began to appear when $\text{C}_2\text{H}_5\text{OH}$ adsorbance was 0.19 mmol/g at TOS = 30 min, which indicated the occurrence of $\text{C}_2\text{H}_5\text{OH}$ adsorbed on open Cr site of Lewis acid. When $\text{C}_2\text{H}_5\text{OH}$ adsorbance reached 0.32 mmol/g at TOS = 55 min, intermolecular dehydration product $\text{C}_2\text{H}_5\text{OC}_2\text{H}_5$ was observed, which indicated that multilayer adsorption of $\text{C}_2\text{H}_5\text{OH}$ on grafted $-\text{OSO}_3\text{H}$ group of Brønsted acid might begin to appear. In the following TOS, selectivity of $\text{C}_2\text{H}_5\text{OC}_2\text{H}_5$ increased with the increasing of $\text{C}_2\text{H}_5\text{OH}$ adsorbance. Equilibrium $\text{C}_2\text{H}_5\text{OH}$ adsorbance of 0.54 mmol/g was reached until TOS = 155 min, another intermolecular product $\text{CH}_3\text{COOC}_2\text{H}_5$ appeared. Results indicated that lower surface $\text{C}_2\text{H}_5\text{OH}$ concentration was conducive to the occurrence of mono-molecular reaction, while higher surface $\text{C}_2\text{H}_5\text{OH}$ concen-

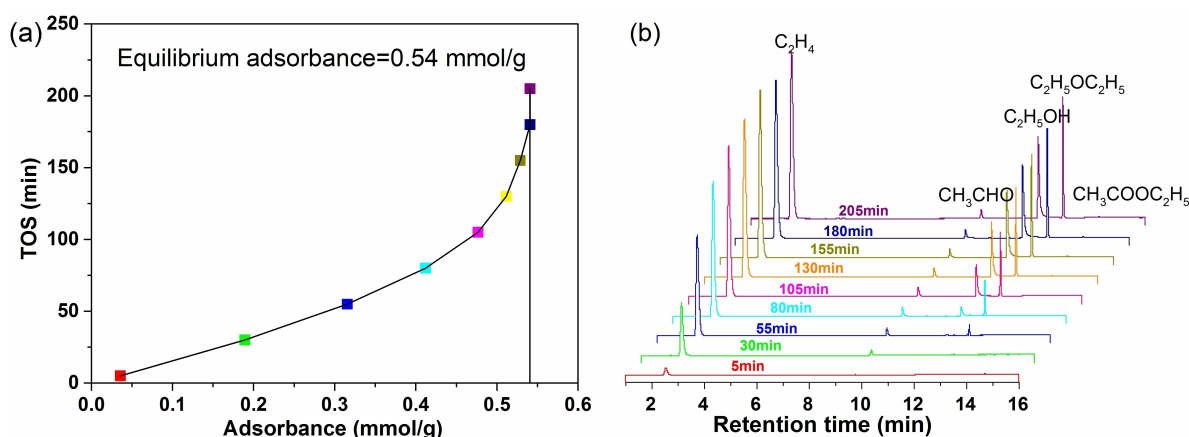


Figure 4. $\text{C}_2\text{H}_5\text{OH}$ adsorbance (a) and product distribution (b) as a function of TOS in the initial stage on HS-MIL-101(Cr) (Reaction temperature = $250\text{ }^\circ\text{C}$, WHSV = 0.02 h^{-1}).

tration was favorable for the occurrence of bi-molecular reaction.

Selective production of C_2H_4 or $C_2H_5OC_2H_5$. By adjusting solution proportion, steam generation temperature and carrier flow, weight hourly space velocity (WHSV) of C_2H_5OH was regulated. In addition, reaction temperature was adjusted purposefully. And the controllable Equilibrium C_2H_5OH adsorbance was achieved finally. Table 3 listed details of steam generation condition and reaction condition. Based on that, selective production in conversion of C_2H_5OH on HS-MIL-101(Cr) was carried out.

Figure 5(a) showed selective production of C_2H_4 in conversion of C_2H_5OH on HS-MIL-101(Cr) at 250 °C. When $WHSV = 0.02 \text{ h}^{-1}$, product distribution was composed of about 60% C_2H_4 , 30% $C_2H_5OC_2H_5$ and 10% CH_3CHO , which testified grafted $-OSO_3H$ group of Brønsted acid and open Cr site of Lewis acid could participate in conversion of C_2H_5OH simultaneously when Equilibrium C_2H_5OH adsorbance was 0.54 mmol/g. With the decreasing of WHSV, C_2H_5OH conversion of 100% and C_2H_4 selectivity of 100% was achieved ultimately when $WHSV = 0.002 \text{ h}^{-1}$, where Equilibrium C_2H_5OH adsorbance was 0.06 mmol/g. Results confirmed that selective production of C_2H_4 in conversion of C_2H_5OH could be tailored when lower surface C_2H_5OH concentration would be satisfied at 250 °C.

Figure 5(b) showed selective production of $C_2H_5OC_2H_5$ in conversion of C_2H_5OH on HS-MIL-101(Cr) at 210 °C. When $WHSV = 0.04 \text{ h}^{-1}$, product distribution was composed of 88% $C_2H_5OC_2H_5$, 5% C_2H_4 and 2% CH_3CHO and 5% $CH_3COOC_2H_5$,

which testified both of mono-molecular and bi-molecular reaction in conversion of C_2H_5OH could take place simultaneously when

Equilibrium C_2H_5OH adsorbance was 1.22 mmol/g. With the increasing of WHSV, $C_2H_5OC_2H_5$ selectivity of 99% with trace CH_3CHO and $CH_3COOC_2H_5$ was achieved when $WHSV = 0.5 \text{ h}^{-1}$, where Equilibrium C_2H_5OH adsorbance was 2.09 mmol/g. Results confirmed that selective production of $C_2H_5OC_2H_5$ in conversion of C_2H_5OH could be tailored when higher surface C_2H_5OH concentration would be satisfied at 210 °C.

Discussion. As a porous material with good designability, MIL-101(Cr) with adjustable Brønsted acid density could be synthesized after post-synthetic sulfation. Possible mechanism in conversion of C_2H_5OH on post-synthesized sulfated MIL-101 (Cr) was proposed, as shown in Scheme 1. Open Cr site of Lewis acid might be dehydrogenation sites, transforming C_2H_5OH to CH_3CHO and further to $CH_3COOC_2H_5$. Grafted $-OSO_3H$ group of Brønsted acid might be dehydration sites, transforming C_2H_5OH to both C_2H_4 and $C_2H_5OC_2H_5$.

C_2H_5OH was preferentially adsorbed on grafted $-OSO_3H$ group of Brønsted acid due to the formation of sulfur-rich surface. Therefore, selectivity of C_2H_4 and $C_2H_5OC_2H_5$ could be effectively improved with the increasing composition of grafted $-OSO_3H$ group of Brønsted acid. As competitive reaction pathways, C_2H_4 was produced dominantly at higher reaction temperature by intramolecular dehydration, while $C_2H_5OC_2H_5$ was produced dominantly at lower reaction temperature by intermolecular dehydration. In addition, surface C_2H_5OH con-

Table 3. Steam generation conditions and reaction conditions in selective production in conversion of C_2H_5OH .

Code	Steam generation condition solution proportion [wt %]	Reaction condition		Equilibrium adsorbance [mmol/g]
		Temp. [°C]	Temp. [°C]	
S-1	10% C_2H_5OH + 90% H_2O	10	250	0.06
S-2	10% C_2H_5OH + 90% H_2O	25	250	0.33
S-3	100% C_2H_5OH	2.5	250	0.54
S-4	100% C_2H_5OH	50	210	1.22
S-5	100% C_2H_5OH	70	210	2.09

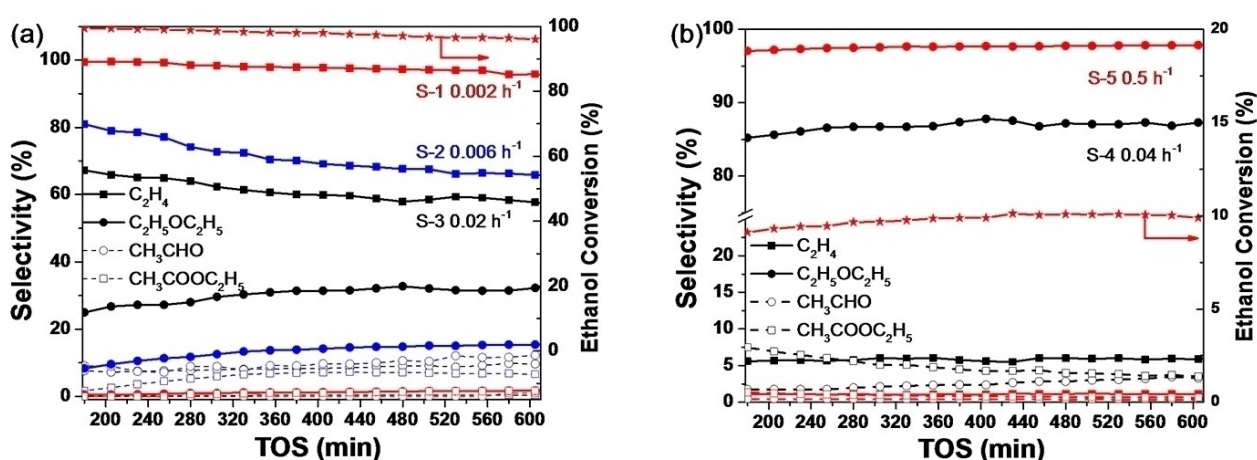
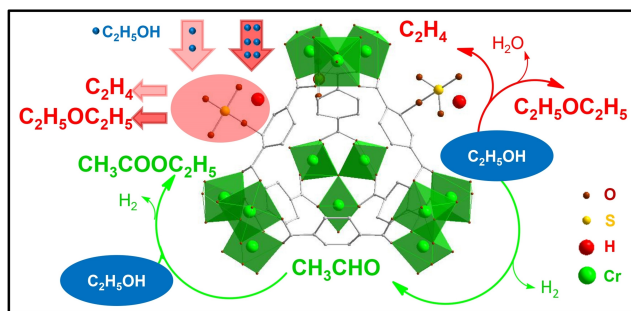


Figure 5. Catalytic performance of selective production in conversion of C_2H_5OH on HS-MIL-101(Cr), (a) 250 °C, (b) 210 °C.



Scheme 1. Schematic diagram of controllable product distribution in conversion of C_2H_5OH on MIL-101(Cr) with adjustable Brønsted acid density.

centration played an important role on the occurrence of mono-molecular reaction and/or bi-molecular reaction. As Scheme 1 shown, the controllable products distribution was achieved on HS-MIL-101(Cr) finally. C_2H_4 selectivity of 100% in conversion of C_2H_5OH could be tailored when lower surface C_2H_5OH concentration would be satisfied at 250 °C. And $C_2H_5OC_2H_5$ selectivity of 99% in conversion of C_2H_5OH could be tailored when higher surface C_2H_5OH concentration would be satisfied at 210 °C.

Fresh and spent MIL-101(Cr) with adjustable Brønsted acid density in conversion of C_2H_5OH at 250 °C for 600 min was compared. XRD patterns (Figure S2) indicated framework integrity was maintained. XPS analysis (Figure S3) and IR spectra (Figure S4) testified no loss of grafted $-OSO_3H$ group. TGA curves (Figure S5) of spent catalysts would be exactly the same as the fresh one, which indicated there was no obvious coke deposition. In this work, the controllable product distribution further confirmed the potential application of designable MOF. Gas-solid catalytic reaction of MIL-101(Cr) was proceeded by continuous feeding, which would provide some reference for its development in real industry application.

Conclusion

MIL-101(Cr) with adjustable Brønsted acid density was synthesized via post-synthetic sulfation strategy. Crystallinity was increased, thermal stability was improved, and higher composition grafted $-OSO_3H$ group of Brønsted acid was located on the surface. Conversion of C_2H_5OH in a micro fixed-bed reactor was adopted as a probe reaction. Open Cr site of Lewis acid might be dehydrogenation sites, transforming C_2H_5OH to CH_3CHO and further to $CH_3COOC_2H_5$. Grafted $-SO_3H$ group of Brønsted acid might be dehydration sites, transforming C_2H_5OH to both C_2H_4 and $C_2H_5OC_2H_5$. With the increasing composition of grafted $-OSO_3H$ group of Brønsted acid, selectivity of C_2H_4 and $C_2H_5OC_2H_5$ could be effectively improved. On HS-MIL-101(Cr), C_2H_4 selectivity of 100% in conversion of C_2H_5OH could be tailored when lower surface C_2H_5OH concentration would be satisfied at 250 °C, and $C_2H_5OC_2H_5$ selectivity of 99% in conversion of C_2H_5OH could be tailored when higher surface C_2H_5OH concentration would be satisfied at 210 °C. Our work

not only found a way to regulate Brønsted acid density, but also confirmed the potential for highly selective catalyst on MOF.

Experimental Section

MIL-101(Cr) was synthesized according to a previous study, and experimental details were described in the Supplementary Information. Post-synthetic sulfation^[25a] was carried out with H_2SO_4 in the presence of $(CF_3SO_2)_2O$ at the molar ratio of 1:1.5 ($n[H_2SO_4]:n[(CF_3SO_2)_2O]=1:1.5$), using CH_3NO_2 as solvent. The mixture was agitated at room temperature. Then the solid was harvested by centrifugation, washed with deionized water and CH_3COCH_3 for three times, dipped in C_2H_5OH for 24 h at 70 °C and dried at 160 °C. Finally, the green powder obtained was denoted as LS-MIL-101(Cr), S-MIL-101(Cr) and HS-MIL-101(Cr), respectively, with the increasing of $n[H_2SO_4]:n[BDC]$. Table 1 summarized sample codes and treatment conditions.

Crystalline structure was analyzed by X-Ray Diffraction (XRD) using PANalytical X'Pert PRO X-ray diffractometer with $Cu K\alpha$ radiation. Scanning electron micrograph was shot by Hitachi SU8020 while Energy Dispersive Spectrometer (EDS) analysis of catalyst surface was conducted with Horiba X-max. The infrared spectra were obtained on a Bruker Vertex 70 FTIR spectrometer in the transmission mode. The samples were mixed with KBr and pressed into discs. Prior to the measurements, the samples were degassed under N_2 at 200 °C for 2 h. X-ray photoelectron spectroscopy (XPS) analysis was conducted with ThermoFisher ESCALAB250xi with monochromatized $Al K\alpha$ as the exciting radiation. Binding energy of C1s at 284.8 eV was used as a reference. Thermogravimetric analysis (TGA) was operated on SDT Q600 under 100 mL/min air at a heating rate of 10 °C/min. Nitrogen sorption isotherms were measured by Micromeritics ASAP 2020 surface area and porosity analyzer at -196.15 °C after degassed at 200 °C for 4 h. Specific BET surface area was computed at 0.05–0.25 relative pressure.

The nature of acidity was measured on Micromeritic Autochem II chemisorption analyzer with a tandem mass spectrometer OmniStar 300. After pretreated under 50 ml/min He at 250 °C for 1 h, the samples were cooled to 100 °C and dosed for 30 min with a 10% NH_3/He . Then, 50 ml/min He was flushed to prevent physisorption of NH_3 . Subsequently, the samples were heated to 250 °C at a heating rate of 10 °C/min. Exhaust gases were analyzed by TCD detector (NH_3 -TPD) and by mass spectrometer tracked the signal $m/z=17$ (NH_3 -TPD-MS). Acid-Base titration was used to determine Brønsted acid density using saturated NaCl solution as an ion-exchange agent.^[35] 0.5 g sample was suspended in 20 g NaCl solution. The mixture was stirred at room temperature for more than 24 h. After standing for another 24 h, the supernatant fluid was collected and titrated with 0.1 M NaOH solution using phenolphthalein as pH indicator.

Catalytic Reaction Experiments. The catalytic reaction was maintained in a quartz tubular fixed-bed reactor, which was placed into a tubular furnace. Before each experiment, fresh catalyst was placed in the middle of the tubular quartz, and quartz wool was used to support the catalyst from both ends. After that, furnace temperature was increased to 250 °C and kept for 180 min under 50 mL/min N_2 to remove impurities. After cooling down to reaction temperature, C_2H_5OH was fed into. Product composition was analyzed using an online GC 7890A equipped with a Polar Plot-Q column.

Acknowledgements

We acknowledge the financial support from the National Natural Science Foundation of China (Grant No. 21878287 and 21576252)

Conflict of Interest

The authors declare no conflict of interests.

Keywords: Adsorption · Dehydration · Dehydrogenation · Alcohol · Acidity

- [1] a) S. Kitagawa, R. Kitaura, S. Noro, *Angew. Chem. Int. Ed.* **2004**, *43*, 2334–2375; *Angew. Chem.* **2004**, *116*, 2388–2430; b) G. Ferey, *Chem. Soc. Rev.* **2008**, *37*, 191–214; c) H. C. Zhou, J. R. Long, O. M. Yaghi, *Chem. Rev.* **2012**, *112*, 673–674.
- [2] a) J. R. Li, R. J. Kuppler, H. C. Zhou, *Chem. Soc. Rev.* **2009**, *38*, 1477–1504; b) S. Ma, H. C. Zhou, *Chem. Commun.* **2010**, *46*, 44–53.
- [3] a) X. Zhao, X. Bu, T. Wu, S. T. Zheng, L. Wang, P. Feng, *Nat. Commun.* **2013**, *4*; b) J. R. Li, J. Sculley, H. C. Zhou, *Chem. Rev.* **2012**, *112*, 869–932.
- [4] a) K. Lu, T. Aung, N. Guo, R. Weichselbaum, W. Lin, *Adv. Mater.* **2018**, *30*; b) Z. Hu, B. J. Deibert, J. Li, *Chem. Soc. Rev.* **2014**, *43*, 5815–5840.
- [5] a) H. Furukawa, K. E. Cordova, M. O’Keeffe, O. M. Yaghi, *Science* **2013**, *341*, 1230444; b) A. Kirchon, L. Feng, H. F. Drake, E. A. Joseph, H. C. Zhou, *Chem. Soc. Rev.* **2018**; c) L. Jiao, Y. Wang, H. L. Jiang, Q. Xu, *Adv. Mater.* **2018**, *30*.
- [6] M. E. Davis, *Nature* **2002**, *417*, 813.
- [7] a) D. Tian, Q. Chen, Y. Li, Y. H. Zhang, Z. Chang, X. H. Bu, *Angew. Chem. Int. Ed.* **2014**, *53*, 837–841; *Angew. Chem.* **2014**, *126*, 856–860; b) M. O’Keeffe, O. M. Yaghi, *Chem. Rev.* **2012**, *112*, 675–702.
- [8] a) J. An, O. K. Farha, J. T. Hupp, E. Pohl, J. I. Yeh, N. L. Rosi, *Nat. Commun.* **2012**, *3*; b) O. M. Yaghi, M. O’Keeffe, N. W. Ockwig, H. K. Chae, M. Eddaoudi, J. Kim, *Nature* **2003**, *423*, 705–714; c) S.-C. Xiang, Z. Zhang, C. G. Zhao, K. Hong, X. Zhao, D. R. Ding, M. H. Xie, C. D. Wu, M. C. Das, R. Gill, K. M. Thomas, B. Chen, *Nat. Commun.* **2011**, *2*; d) L. Liu, K. Konstas, M. R. Hill, S. G. Telfer, *J. Am. Chem. Soc.* **2013**, *135*, 17731–17734.
- [9] X. Lin, I. Telepeni, A. J. Blake, A. Dailly, C. M. Brown, J. M. Simmons, M. Zoppi, G. S. Walker, K. M. Thomas, T. J. Mays, P. Hubberstey, N. R. Champness, M. Schroeder, *J. Am. Chem. Soc.* **2009**, *131*, 2159–2171.
- [10] a) G. Ferey, C. Mellot-Draznieks, C. Serre, F. Millange, J. Doutour, S. Surble, I. Margiolaki, *Science* **2005**, *309*, 2040–2042; b) O. K. Farha, A. O. Yazaydin, I. Eryazici, C. D. Malliakas, B. G. Hauser, M. G. Kanatzidis, S. T. Nguyen, R. Q. Snurr, J. T. Hupp, *Nat. Chem.* **2010**, *2*, 944–948.
- [11] A. Aijaz, A. Karkamkar, Y. J. Choi, N. Tsumori, E. Roennebro, T. Autrey, H. Shioyama, Q. Xu, *J. Am. Chem. Soc.* **2012**, *134*, 13926–13929.
- [12] a) M. Yoon, R. Srirambalaji, K. Kim, *Chem. Rev.* **2012**, *112*, 1196–1231; b) C. Zhu, G. Yuan, X. Chen, Z. Yang, Y. Cui, *J. Am. Chem. Soc.* **2012**, *134*, 8058–8061.
- [13] a) X. Xu, J. A. van Bokhoven, M. Ranocchiari, *ChemCatChem* **2014**, *6*, 1887–1891; b) M. C. Das, S. Xiang, Z. Zhang, B. Chen, *Angew. Chem. Int. Ed.* **2011**, *50*, 10510–10520; *Angew. Chem.* **2011**, *123*, 10696–10707.
- [14] B. L. Chen, M. Eddaoudi, T. M. Reineke, J. W. Kampf, M. O’Keeffe, O. M. Yaghi, *J. Am. Chem. Soc.* **2000**, *122*, 11559–11560.
- [15] M. Vandichel, F. Vermoortele, S. Cottenie, D. E. De Vos, M. Waroquier, V. Van Speybroeck, *J. Catal.* **2013**, *305*, 118–129.
- [16] A. Henschel, K. Gedrich, R. Kraehnert, S. Kaskel, *Chem. Commun.* **2008**, 4192–4194.
- [17] a) N. V. Maksimchuk, M. N. Timofeeva, M. S. Melgunov, A. N. Shmakov, Y. A. Chesalov, D. N. Dybtsev, V. P. Fedin, O. A. Kholdeeva, *J. Catal.* **2008**, *257*, 315–323; b) J. Kim, S. Bhattacharjee, K. E. Jeong, S. Y. Jeong, W. S. Ahn, *Chem. Commun.* **2009**, 3904–3906; c) N. V. Maksimchuk, K. A. Kovalenko, V. P. Fedin, O. A. Kholdeeva, *Adv. Synth. Catal.* **2010**, *352*, 2943–2948.
- [18] J. Jiang, O. M. Yaghi, *Chem. Rev.* **2015**, *115*, 6966–6997.
- [19] W. Salomon, C. Roch Marchal, P. Mialane, P. Rouschmeyer, C. Serre, M. Haouas, F. Taulelle, S. Yang, L. Ruhlmann, A. Dolbecq, *Chem. Commun.* **2015**, *51*, 2972–2975.
- [20] V. G. Ponomareva, K. A. Kovalenko, A. P. Chupakhin, D. N. Dybtsev, E. S. Shutova, V. P. Fedin, *J. Am. Chem. Soc.* **2012**, *134*, 15640–15643.
- [21] J. Jiang, F. Gandara, Y. B. Zhang, K. Na, O. M. Yaghi, W. G. Klemperer, *J. Am. Chem. Soc.* **2014**, *136*, 12844–12847.
- [22] W. Morris, C. J. Doonan, O. M. Yaghi, *Inorg. Chem.* **2011**, *50*, 6853–6855.
- [23] a) M. L. Foo, S. Horike, T. Fukushima, Y. Hijikata, Y. Kubota, M. Takata, S. Kitagawa, *Dalton Trans.* **2012**, *41*, 13791–13794; b) J. Juan Alcaniz, R. Gielisse, A. B. Lago, E. V. Ramos Fernandez, P. Serra Crespo, T. Devic, N. Guillou, C. Serre, F. Kapteijn, J. Gascon, *Catal. Sci. Technol.* **2013**, *3*, 2311–2318; c) Y. X. Zhou, Y. Z. Chen, Y. L. Hu, G. Huang, S. H. Yu, H. L. Jiang, *Chem. Eur. J.* **2014**, *20*, 14976–14980.
- [24] a) S. Biswas, J. Zhang, Z. Li, Y. Y. Liu, M. Grzywa, L. Sun, D. Volkmer, P. Van der Voort, *Dalton Trans.* **2013**, *42*, 4730–4737; b) L. Wang, M. Yang, Z. Shi, Y. Chen, S. H. Feng, *J. Solid State Chem.* **2005**, *178*, 3359–3365; c) C. Qin, X. L. Wang, L. Carlucci, M. L. Tong, E. B. Wang, C. W. Hua, L. Xua, *Chem. Commun.* **2004**, 1876–1877.
- [25] a) M. G. Goesten, J. Juan Alcaniz, E. V. Ramos Fernandez, K. B. S. S. Gupta, E. Stavitski, H. van Bekkum, J. Gascon, F. Kapteijn, *J. Catal.* **2011**, *281*, 177–187; b) S. Yuan, L. Feng, K. C. Wang, J. D. Pang, M. Bosch, C. Lollar, Y. J. Sun, J. S. Qin, X. Y. Yang, P. Zhang, Q. Wang, L. F. Zou, Y. M. Zhang, L. L. Zhang, Y. Fang, J. L. Li, H. C. Zhou, *Adv. Mater.* **2018**, *30*, 35.
- [26] U. Olsbye, S. Svelle, M. Bjorgen, P. Beato, T. V. W. Janssens, F. Joensen, S. Bordiga, K. P. Lillerud, *Angew. Chem. Int. Ed.* **2012**, *51*, 5810–5831; *Angew. Chem.* **2012**, *124*, 5910–5933.
- [27] M. H. Zhang, Y. Z. Yu, *Ind. Eng. Chem. Res.* **2013**, *52*, 9505–9514.
- [28] a) J. W. Liu, L. F. Chen, H. Cui, J. Y. Zhang, L. Zhang, C. Y. Su, *Chem. Soc. Rev.* **2014**, *43*, 6011–6061; b) A. U. Czaja, N. Trukhan, U. Mueller, *Chem. Soc. Rev.* **2009**, *38*, 1284–1293.
- [29] L. Ye, *Nat. Gas Chem. Ind.* **2018**, *43*, 126–132.
- [30] T. Y. Xie, K. B. McAuley, J. C. C. Hsu, D. W. Bacon, *Ind. Eng. Chem. Res.* **1994**, *33*, 449–479.
- [31] T. Kito Borsari, D. A. Pacas, S. Selim, S. W. Cowley, *Ind. Eng. Chem. Res.* **1998**, *37*, 3366–3374.
- [32] a) J. Wang, R. Huang, Y. J. Zhang, J. Y. Diao, J. Y. Zhang, H. Y. Liu, D. S. Su, *Carbon* **2017**, *111*, 519–528; b) J. Sun, Y. Wang, *ACS Catal.* **2014**, *4*, 1078–1090.
- [33] a) D. S. Warren, A. J. McQuillan, *J. Phys. Chem. B* **2008**, *112*, 10535–10543; b) P. Atorngitjawat, R. J. Klein, J. Runt, *Macromolecules* **2006**, *39*, 1815–1820.
- [34] B. Ostrowskagumkowska, *Eur. Polym. J.* **1994**, *30*, 875–879.
- [35] S.-Y. Chen, T. Yokoi, C.-Y. Tang, L.-Y. Jang, T. Tatsumi, J. C. C. Chan, S. Cheng, *Green Chem.* **2011**, *13*, 2920–2930.

Manuscript received: August 18, 2020

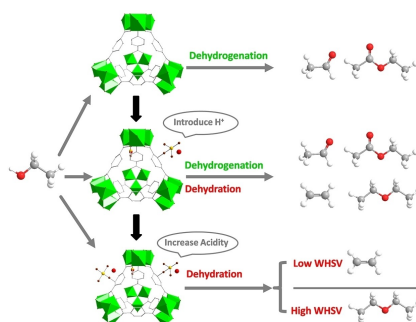
Revised manuscript received: September 18, 2020

Accepted manuscript online: September 22, 2020

Version of record online: ■■■, ■■■■

FULL PAPERS

Product control: In conversion of C_2H_5OH on MIL-101(Cr) with adjustable Brønsted acid density, open Cr site of Lewis acid as dehydrogenation sites results in the transformation of C_2H_5OH to CH_3CHO and further to $CH_3COOC_2H_5$; and grafted $-OSO_3H$ group of Brønsted acid as dehydration sites could convert C_2H_5OH to both C_2H_4 and $C_2H_5OC_2H_5$. Additionally, selectivity of products can be tailored by surface C_2H_5OH concentration.



Z. Ming, Prof. Y. Wang, Prof. T. Zhang,
L. Li, Prof. C. Duan*, Prof. Z. Liu*

1 – 8

**Product Control in Conversion of
Ethanol on MIL-101(Cr) with Adjustable Brønsted Acid Density**

